**Atmospheric
Chemistry
and Physics
Discussions**

Diagnosing climate
sensitivity from
fluctuations

D. Kirk-Davidoff

Title Page

Abstract	Introduction
Conclusions	References
Tables	Figures

|◄ | ►|
◄ | ►
Back | Close

Full Screen / Esc

Printer-friendly Version

Interactive Discussion

On the diagnosis of climate sensitivity using observations of fluctuations

D. Kirk-Davidoff

Department of Atmospheric and Oceanic Science, University of Maryland, College Park, MD 20742, USA

Correspondence to: D. Kirk-Davidoff (dankd@atmos.umd.edu)

Abstract

It has been shown that lag-covariance based statistical measures, suggested by the Fluctuation Dissipation Theorem (FDT), may allow estimation of climate sensitivity in a climate model. Recently Schwartz (2007) has used measures of the decay of autocorrelation in a global surface temperature time series to estimate the real world climate sensitivity. Here we use a simple climate model, and analysis of archived coupled climate model output from the IPCC AR runs, for which the climate sensitivity is known, to test the utility of this approach. Our analysis of archived data show that estimates of climate sensitivity derived from century-long time scales typically grossly underestimate the models' true climate sensitivity. We analyze the behavior of the simple model with adjustable heat capacity in two surface layers, subject to various stochastic forcings and for various climate sensitivities, modulated by albedo and water vapor feedbacks. We use our simple climate model to demonstrate:

1. that a much longer time series would be required to accurately diagnose the earth's climate sensitivity than is presently available,

2. that for shorter time series there is a systematic bias towards underpredicting climate sensitivity,

3. that the addition of a second heat reservoir weakly coupled to the first greatly reduces the decorrelation timescale of short temperature time series produced by the model, aggravating the tendency to underestimate climate sensitivity, and

4. that because of this it is possible to have a selection of models in which the climate sensitivity is inversely related to the decorrelation time scale, as is true for the IPCC models.

1 Introduction

Leith (1975) and Bell (1980) introduced the idea that the climate sensitivity of the earth or of a general circulation model (GCM) could be predicted using the Fluctuation Dissipation Theorem (FDT) (Callen and Green, 1952). The FDT states that for systems near equilibrium, the rate at which anomalies dissipate is related the sensitivity of the system to a finite change in forcing. Bell (1980) and Cionni et al. (2004) were able to show that global climate sensitivity could in fact be predicted to useful accuracy for a simplified climate model and for a highly complex chemical GCM, respectively using measures based on the FDT, depending on the lag-autocorrelation matrix of the model temperature. Langen and Alexeev (2005) used the FDT to predict the zonal mean response of a GCM to climate forcing, using 500 yr of model output data. North et al. (1993) and von Storch (2004) considered the dissipation of fluctuations in a GCM and discussed the applicability of the FDT to climate models. Great hopes have been staked on the use of the FDT to diagnose sensitivity using satellite infrared radiance data (Goody et al., 1998).

In all of these discussions, two aspects of the potential use of the FDT for climate sensitivity diagnoses have been neglected. First, there has been no explicit discussion of the use of the FDT in the case where the heat capacity of the system is uncertain. Second, there has been no thorough investigation of how the length of the time series needed for an accurate diagnosis of climate sensitivity depends on the parameters (climate sensitivity, heat capacity, number of independent variables) of the system. In this paper, we investigate the practical usefulness of the FDT for the purpose of diagnosing climate sensitivity. To do so, we use an extremely simple climate model that is nevertheless includes parameters controlling climate sensitivity, heat capacity and internal heat transports.

More recently, Schwartz (2007) has used analysis of lag-autocorrelation of the global mean surface temperature time series for the last 150 yr along with analysis of ocean heat storage over the last 50 yr, to simultaneously calculate the earth's effective heat

Diagnosing climate sensitivity from fluctuations

D. Kirk-Davidoff

⏮ | ⏭

◀ | ▶

Back | Close

Full Screen / Esc

Printer-friendly Version

Interactive Discussion

capacity and climate sensitivity. Schwartz (2007) diagnosed a value of the climate sensitivity ($\approx 0.3\,\mathrm{K\,W^{-1}\,m^2}$) that was quite low compared to other estimates of climate sensitivity ($\approx 0.75\,\mathrm{K\,W^{-1}\,m^2}$). Schwartz argued that the discrepancy was due to the models' over-estimate of the climate system's decorrelation time scale, arguing that while his results showed a decorrelation time scale of about 5 yr, climate models typically required some 30 yr to fully adjust to a step change in climate forcing. We will show that actual climate model time series typically show decorrelation time scales similar to that found by Schwartz (2007) for observed global average surface air temperature. Thus, application of Schwartz's technique to climate model output results in a substantial underestimate of the climate models' climate sensitivity. We will use a simple heuristic climate model to show how a model with a relatively long adjustment time may nevertheless exhibit a short decorrelation time-scale.

In Sect. 2 we review the use of lag-correlation analysis to estimate climate sensitivity. In Sect. 3, we apply Schwartz (2007)'s method to the IPCC AR4 model runs, to test the method on modeled climate systems whose climate sensitivity is known. In Sects. 4 and 5 we introduce our simple climate model and apply it to explain the systematic underestimate of climate sensitivity by the lag-correlation method. These errors are due both to the inadequate length of the time series involved, and to the assumption of a single heat capacity for the climate system.

"Note added in proof: the author has recently become of aware of three comments on Schwartz (2007), some of which overlap with material in this paper (Foster et al., 2008; Knutti et al., 2008; Scafetta, 2008), and a reply (Schwartz, 2008). In particular, Knutti et al. (2008) perform a similar analysis of the IPCC model output data, with similar results."

1.1 Fluctuation dissipation and climate sensitivity

To gain an intuitive understanding of the use of lag-correlation techniques to estimate climate sensitivity, the reader should imagine the climate system as a linear oscillator. By observing unforced oscillations of the temperature, we hope to estimate the

response of the climate system to a step change in climate forcing. We assume that the unforced fluctuations, though in reality driven by internal instabilities, can be treated as though they were driven by random fluctuations of the forcing. The system tends to return to its equilibrium temperature because of the dominant blackbody feed-
5　back, whereby an increase in temperature leads to an increase in outgoing radiation, and thus a return to equilibrium. Thus, in a system with large climate sensitivity, a small fluctuation in forcing leads to feedbacks that tend to slow the return of the system to equilibrium. On the other hand, in a system with small climate sensitivity the same fluctuation in forcing causes a smaller temperature change, and thus a more
10　rapid return to equilibrium. Thus a time series of surface temperature ought to show larger lag-autocorrelation in the system with larger climate sensitivity, and smaller lag-autocorrelation in the system with smaller climate sensitivity.

There are a number of reasons to suspect that this relationship might not be so simple in the real world. The relative importance of external and internal drivers of
15　global temperature is different at different time scales, and it is reasonable to suppose that feedbacks might therefore act differently at different time scales. For instance, interannual variations of global mean surface temperature in the real climate system are largely driven by internal oscillations of the system (e.g. ENSO), where the mean temperature change is a small residual of large and nearly compensating patterns of
20　heating and cooling. In this case it is clear that any geographic dependence in the strength of climate feedbacks might make the global feedback have a different relationship to the global temperature for these internally forced variations than for externally forced climate change (e.g. by a secular trend in carbon dioxide concentration).

Keeping these caveats in mind, we now formalize our treatment of the relationship
25　between the lag-correlation and climate sensitivity for a purely linear system. Our discussion follows that of Penland and Sardeshmukh (1995). Consider a linear system forced by white noise ($\boldsymbol{\xi}$) and a fixed forcing $\boldsymbol{f}$:

$$\frac{d\boldsymbol{x}}{dt} = \mathbf{B}\boldsymbol{x} + \boldsymbol{\xi} + \boldsymbol{f},$$
(1)

Diagnosing climate sensitivity from fluctuations

D. Kirk-Davidoff

ı◀ | ▶ı

◀ | ▶

Back | Close

Full Screen / Esc

Printer-friendly Version

Interactive Discussion

A change in f from f_0 to f_1 will result in a change in the long-term mean value of x of $(\bar{x}_1 - \bar{x}_0) = -\mathbf{B}^{-1}(f_1 - f_0)^{-1}$. Thus we call $-\mathbf{B}$ the sensitivity matrix. $-\mathbf{B}$ can be determined by observation of the lag-covariances of the system, as follows:

$$\mathbf{B} = \frac{1}{\tau} \ln \mathbf{C}_{xx}(\tau)\mathbf{C}(0)^{-1}, \tag{2}$$

where $\mathbf{C}_{xx}(\tau) = <x(t+\tau)x^T(t)>$, and τ is an arbitrary time lag. By taking the exponent of both sides of Eq. (2), and then integrating over all time lags τ, one obtains

$$\int_0^\infty \exp(\tau \mathbf{B})d\tau = \int_0^\infty \mathbf{C}(\tau)\mathbf{B}(0)^{-1}d\tau \tag{3}$$

or

$$-\mathbf{B}_{est}^{-1} = \int_0^\infty \mathbf{C}(\tau)\mathbf{C}(0)^{-1}d\tau, \tag{4}$$

which is a form of the FDT. Note that no use is made in this estimate of the white noise forcing, ξ, and that the sensitivity is given in units of time: it is the time scale of the equivalent restoring force of the system. In any practical application of the FDT to climate sensitivity diagnosis, we must assert that the climate system can be approximated by a system like Eq. (1), and we must be able the calculate the forcing in units of Kelvins per unit time. This requires independent knowledge of the heat capacity of the climate system.

One can use either Eqs. (2) or (4) to obtain $\mathbf{B}$. Schwartz (2007) used a scalar equivalent to Eq. (1), to estimate the relaxation time constant for the time series of global mean temperature, $-\frac{1}{\tau}\ln c(\tau)$, by plotting its value versus τ for lags of up to 20 yr, and looking for a tendency of the value of the relaxation time constant to asymptote to a fixed value as τ increased. He combined this estimate with a separate estimate of global heat capacity to produce his estimate of climate sensitivity.

Diagnosing climate sensitivity from fluctuations

D. Kirk-Davidoff

Cionni et al. ([2004](#)) employed a method inspired by the FDT, where instead of calculating the integral of the lag covariance matrix of the system x, they calculated the integral of the lag covariance of the system x and the forcing ξ:

$$-\mathbf{B}_{est}^{-1} = \int_0^{\tau_L} \mathbf{R}_{x\xi}(\tau)d\tau, \tag{5}$$

5   where

$$\mathbf{R}_{x\xi}(\tau) = \int_0^\infty x(t+\tau)\xi(t)^T dt \Big/ \int_0^\infty \xi(t)\xi(t)^T dt. \tag{6}$$

τ_L, the upper limit of integration in Eq. ([5](#)) is the lag beyond which no significant correlation is observed. One way to choose a value for this variable is to integrate Eq. ([5](#)) for a sufficiently large τ_L that $\mathbf{B}_{est}$ reaches a maximum, and then begins to decrease. Cionni
10   et al. ([2004](#)) accurately estimated climate sensitivity based on a 10 yr time series of model output data from a GCM run with fixed surface temperature and known forcings. In their study, diagnosis of effective heat capacity was not needed because only the small land surface heat capacity contributed to the decorrelation time. In the real world the task becomes more difficult, due to short time series and a lack of accurate forcing
15   information.

2   Application to IPCC AR4 model output

Here we apply the tools described above to test the ability of analysis based on lag-correlation of temperature timeseries, combined with estimation of global heat capacity by the methods of Schwartz ([2007](#)) to predict climate sensitivity in the IPCC AR4
20   model runs. Figure [1](#)a shows the autocorrelation of the detrended global mean surface air temperature as function of lag (in years) for 18 coupled model simulations of the 20th century (the "20c3m" runs). The three curves shown in blue are three models arbitrarily selected for having longer decorrelation time scales, while the three red curves

have shorter decorrelation time scales. The curve for the GISS global mean surface air temperature (Hansen et al., 1996) is shown in light blue, and is the same curve shown in Schwartz (2007), Fig. 2c. Note the good agreement between the GISS curve and the IPCC model curves. Figure 1b shows the relaxation time constant, $-\frac{1}{\tau}\ln c(\tau)$

5 for the same global mean surface air temperature time series. Again, the light blue curve showing the GISS observations falls well within the range of the IPCC model lag autocorrelation curves. We calculate the model relaxation time scale by finding the lag for which the autocorrelation is less than zero, and averaging the relaxation time scale either over all lags up to the lag with zero correlation, or the relaxation over the three

10 years prior to that lag, whichever is greater. Using this method, the average relaxation time scale for the models is 8.3 yr, with a standard deviation of 4.5 yr, and a range of 2.8–18.5 yr. Thus, Schwartz (2007)'s estimate of 5 yr falls in the range of the model relaxation time scales.

Following Schwartz (2007) we calculate the models' effective heat capacity using two

15 methods: by regressing the global heat storage against the global temperature, and by taking the ratio of the trends of heat storage and temperature. Heat storage is obtained by integrating the global downward flux of heat at the atmosphere's lower boundary, which is the sum of the latent and sensible heat fluxes, and the net downward long and shortwave fluxes. Scatter plots of annual and global mean heat storage anomaly

20 versus annual and global mean temperature anomaly are shown in Fig. 2, offset from zero mean for clarity. The light blue points refer the observed ocean heat storage, and were taken by digitizing the lower right panel of Fig. 4 in Schwartz (2007). That figure plots GISS surface temperatures against ocean heat storage from the surface to 3000 m from the Levitus data set (Levitus et al., 2005), scaled upwards to account

25 for the heat capacity of land. It is apparent that the slope of the dependence of heat storage on surface temperature (shown in light blue) for the observed data is small ($12\,\mathrm{W\,yr\,m^{-2}}$) compared to the range of values found for the models. The average slope for the model data is $90\,\mathrm{W\,yr\,m^{-2}\,K^{-1}}$, with a minimum of $10\,\mathrm{W\,yr\,m^{-2}\,K^{-1}}$, and a standard deviation of $81\,\mathrm{W\,yr\,m^{-2}\,K^{-1}}$.

Diagnosing climate sensitivity from fluctuations

D. Kirk-Davidoff

Full Screen / Esc

Printer-friendly Version

Interactive Discussion

With these two quantities calculated, we can now, following Schwartz (2007), make an estimate of the equilibrium climate sensitivity, and see how well it predicts the actual model sensitivity. One difficulty with this procedure concerns the definition of climate sensitivity. Since the theory underlying the use of the decorrelation time scale to predict climate sensitivity assumes a linear model of climate dynamics, the estimate ought to work best for a very small climate forcing perturbation. However, for reasons of practical interest, climate models are generally run for finite periods using finite forcing. For the IPCC AR4 coupled model runs, we can define climate sensitivity as either:

1. the full response to a doubling of carbon dioxide, where the doubling occurs over a period of 150 yr, and the models are then run for an additional 100 yr allowing an approximate allowing an approximate equilibration,

2. as the transient response during a 1 percent per year increase of carbon dioxide, or

3. as the transient response to one of several particular emission scenarios in which a range of greenhouse gases increase monotonically over the course of the model runs.

In Fig. 3, we show that these sensitivities are related but different. Here, transient sensitivity of the models (in K/100 yr) derived from a linear fit to the trend of global mean temperature for the first 50 yr of runs with carbon dioxide increasing 1% yr^{-1} is compared with climate sensitivity derived from the temperature difference for the years 2000 to 2100 in the "SRESa1b" climate forcing scenario. Among the nineteen models with output for both experiments stored in the PCMDI archive, the correlation coefficient of these two measures of climate sensitivity is 0.57, indicating that important aspects of the climate system (whether the effective climate forcing due to the imposed changes in greenhouse gas forcing, the climate feedbacks or the effective heat capacities of different components of the climate system) respond differently to these two forcing scenarios. In the following discussion we will present results comparing the climate

Full Screen / Esc

Printer-friendly Version

Interactive Discussion

sensitivity derived using the procedure of Schwartz (2007) with the transient climate response of the models in the 1% yr^{-1} forcing scenario. The reader should note however, that similar comparisons have been done with the SRESa1b-derived sensitivities, with broadly similar results (not shown).

5   In Fig. 4a, we confirm that the estimates of global effective heat capacity derived from regression of global heat storage against global heat temperature in the 20c3m model runs are reasonably well correlated ($r=0.70$) with the estimates derived from the ratio of the trends of the two numbers. Heat capacity is shown in units of equivalent mixed layer depth (m), calculated by dividing the heat storage per unit area by

10   the heat capacity of 1 m^3 of sea water. Having established this, we proceed using the average of the two methods. Figure 4b shows the relationship between the decorrelation time scale and the effective global heat capacity. Contrary to the prediction of a linear, single heat reservoir theory of climate dynamics, the relationship is weak, and anticorrelated ($r=-0.48$): models with large decorrelation time scales tend to have

15   small heat storage. When we compare decorrelation time with model sensitivity derived from the first 100 yr of the SRESa1b runs (Fig. 4c), the correlation is very weak and marginally negative ($r=-0.20$). Finally we compare the estimate of climate sensitivity calculated by dividing the decorrelation timescale by the effective heat global heat capacity, as calculated by Schwartz (2007). We find that the estimate of climate sensitivity

20   made by Schwartz (0.30 K W^{-1} m^2) fall squarely within the range of climate sensitivity derived from the IPCC AR4 models (mean=0.22 K W^{-1} m^2, min=9.9×10^{-4} K W^{-1} m^2, max=1.8 K W^{-1} m^2). When the estimated climate sensitivity is compared with the actual climate sensitivity derived from the SRESa1b runs (Fig. 4d), the relationship is, again, weak and negative ($r=-0.18$).

25   These results show that contra Schwartz (2007), the decorrelation time scale of the global mean temperature time series is not in conflict with the range of model estimates, but that the global effective heat capacity is overestimated by the great majority of the IPCC AR4 models. Since climate sensitivity is predicted by simple linear theory to be equal to the decorrelation time scale divided by the ocean heat uptake, excessive

heat uptake combined with a realistic decorrelation timescale should lead the models to underestimate climate sensitivity. However, the fact that the models themselves do not obey this relationship (i.e. the ratio of decorrelation time scale over effective heat capacity is slightly negatively correlated with model climate sensitivity) is a strong
5 argument against the use of the simple linear theory to estimate the earth's climate sensitivity. In the next two sections we use a very simple model of the climate system to explore why the theory might fail for climate system models, and for the real climate system.

3 Model description

10 For simplicity and ease of integration, we make use of a global mean climate model with a single atmospheric layer and purely radiative interactions between the surface and the atmosphere. The features needed include rapid integration, an ability to simulate arbitrary climate sensitivity, and simulation of both radiative and dynamical energy fluxes. The model includes two ocean mixed layers (upper and lower) with an ad-
15 justable linear coupling, to simulate heat storage in the ocean, a single atmospheric layer to account for greenhouse warming, and gray-body radiation. Feedbacks include a temperature-dependent atmospheric infrared emissivity (intended to represent the water vapor feedback), and a temperature-dependent surface albedo (intended to represent ice-albedo and low cloud feedbacks). The model is forced with modified red
20 noise applied to either the solar variability or the infrared emissivity.

The thermodynamic equations for the lower and upper mixed layers, and for the atmosphere are:

$$C_{s2}\frac{dT_{s2}}{dt} = -\gamma(T_s - T_{s2}) \tag{7}$$

$$C_s\frac{dT_s}{dt} = -\gamma(T_{s2} - T_s) + \frac{1}{4}S(1 - \epsilon_S)(1 - \alpha) - \sigma T_s^4 + \epsilon\sigma T_a^4 \tag{8}$$

$$C_a \frac{dT_a}{dt} = \frac{1}{4} \epsilon_S S(1 + \alpha) + \epsilon \sigma T_s^4 - 2\epsilon \sigma T_a^4 \qquad (9)$$

where C_s and C_{s2} are the heat capacities of the upper and lower mixed layers, T_s and T_{s2} are their respective temperatures, C_a and T_a are the heat capacity and temperature of the atmosphere, γ is the coupling time constant between the upper and lower mixed layers, S is the solar constant, ϵ_S is the solar absorption of the atmosphere, α is the surface albedo, σ is the Stefan-Boltzmann constant, and ϵ is the infrared emissivity of the atmosphere.

The atmospheric emissivity and the surface albedo are subject to linear feedbacks on atmospheric and surface temperature, respectively:

$$\epsilon = \epsilon_0 + f_\epsilon(T_a - T_\epsilon) + c_\epsilon A_\epsilon \qquad (10)$$

$$\alpha = \alpha_0 + f_\alpha(T_s - T_\alpha) \qquad (11)$$

where ϵ_0 and α_0 are the basic state emissivity and surface albedo, respectively, T_ϵ and T_α are the basic state atmosphere and surface temperatures, respectively, and f_ϵ and f_α are the feedback parameters. A_ϵ is a red-noise forcing, and c_α is a constant that controls its magnitude. The solar constant can also be forced with red noise:

$$S = S_0 + c_S A_S, \qquad (12)$$

where c_S is a constant controlling the magnitude of the forcing. A_ϵ and A_S are generated using:

$$x_{i+1} = \beta x_i + r \qquad (13)$$

$$A = \left[x - \frac{1}{2(1 - \beta)} \right] \sqrt{1 - \beta^2} \qquad (14)$$

where r is a random variable with a flat distribution over the range [0 1], β is the parameter that determines the autocorrelation of the red-noise forcing, and the scaling is performed after x has been calculated for as many time steps as necessary.

Diagnosing climate sensitivity from fluctuations

D. Kirk-Davidoff

|◄ | ►|

◄ | ►

Back | Close

Full Screen / Esc

Printer-friendly Version

Interactive Discussion

Solving Eqs. (7)–(9) for equilibrium conditions, with feedbacks and stochastic forcing assumed to be zero yields

$$T_s = \sqrt[4]{\frac{S_0[1 - \alpha + \frac{e_s}{2}(3\alpha - 1 - e_s\alpha)]}{\sigma(1 - \frac{e}{2})}} \tag{15}$$

$$T_a = \sqrt[4]{\frac{1}{2}T_s^4 + e_s\frac{S_0}{4}\frac{1 + \alpha - e_s\alpha}{2e\sigma}} \tag{16}$$

Figure 5a shows the equilibrium climate sensitivity of the surface temperature for a range of feedback parameter settings, when the solar constant is increased from $1360\,\mathrm{W\,m^{-2}}$ to $1370\,\mathrm{W\,m^{-2}}$. Depending on the values of the parameter settings, the climate sensitivity for this forcing varies from 0.04 to $1.6\,\mathrm{K\,W^{-1}\,m^2}$, where the surface temperature has been divided by the change in solar forcing adjusted for albedo and geometry, $\frac{\Delta S}{4}(1 - \alpha)$.

Figure 5b shows that as the feedback parameters increase, the time required for the temperature to reach 90% of its equilibrium value is increased. This increase appears at first glance to be very similar to that of the climate sensitivity. However, as shown in Fig. 5c, the ratio of the response time to the climate sensitivity is not constant, but increases with increasing emissivity feedback. This lack of proportionality of the climate sensitivity and the adjustment timescale is due to the fact that the emissivity feedback parameter acts on T_a, rather than on T_s. For a lag-autocorrelation based methodology to accurately predict the climate sensitivity, the fluctuations of both T_a and T_s would have to be observed. Nevertheless, for a modest range of possible climate sensitivities (e.g. over a factor of 3), the ratio of the climate sensitivity to the adjustment time varies only by about 20%. The more serious obstacles to the use of lag-autocorrelations to predict sensitivity arise from the possibility of multiple heat reservoirs, as we discuss in the next section.

4 Simple model results and sensitivity experiments

We now turn to the results of a series of experiments designed to show how statistics like those used by Schwartz (2007) can give misleading results about climate sensitivity. Figure 6 shows the simple model's response to changes in the solar constant. In Fig. 6a, the solar constant is increased by step change of $10\,\mathrm{W\,m^{-2}}$. The feedback parameters are set to $f_e = 0.002\,\mathrm{K^{-1}}$ and $f_\alpha = 0.002\,\mathrm{K^{-1}}$. Three settings for heat capacity are compared: a single ocean mixed layer 25 m deep, a single layer 1000 m deep, and an upper layer of 25 m coupled to a lower layer of 1000 m, with a coupling constant of $50\,\mathrm{W\,m^{-2}\,K^{-1}}\,\mathrm{s}-1$. Note that the relaxation time scale of the coupled case is identical to that of the 1000 m mixed layer case, except that there is an initial rapid approach to equilibrium in the time scale of the upper 25 m layer before the coupling between the layers acts to move the heat to the lower layer. In Fig. 6b, the solar constant varies randomly for the same parameter settings. The rapid oscillations of the coupled case indicates that the shallow upper mixed layer controls the time scale of the response. This behavior suggests that a diagnostic method based on decorrelation time scale will have trouble distinguishing between a system with low heat capacity on short time scales and one with low heat capacity on all time scales.

Pursuing this thread of argument, we now apply Schwartz (2007)'s methodology to much longer synthetic time series, in order to test its ability to extract the model's true dynamics from finite time series. Figure 7 shows the lag autocorrelation $r(\Delta t)$ for two model parameter settings. Figure 7a shows results for a single 25 m mixed layer. Figure 7b shows results for a 25 m mixed upper layer, and a 1000 m mixed lower layer. In each case, the model was run for 10 000 yr, forced by white noise solar variability, and the time series of annual mean T_s was calculated. Red curves show $r(\Delta t)$ calculated separately for 100 100-year chunks of data. The black curve shows $r(\Delta t)$ calculated for the full 10 000 yr record. These results demonstrate two key points.

First, the uncertainty with which one can establish the value of the autocorrelation of a given 100 yr time series is not the relevant uncertainty for the calculation of climate

sensitivity. It is clear from panel Fig. 7a that a single curve of autocorrelation versus lag derived from a 100 yr time series can give only a poor estimate of the true curve. For instance, while the autocorrelation curve derived from the 10 000 yr time series crosses zero at 10 yr lag, the mean of the 100 yr autocorrelation curves' zero crossing is 8.4 yaers, with a standard deviation of 5.7 yr. Even for a model with a single heat capacity, analysis of the lag-autocorrelation of hundred year temperature time series results in both large negative bias in estimating the true decorrelation time scale ($-\Delta t / \ln(r(\Delta t)$, averaged over lags from 8 to 12 yr), and large variance of the decorrelation time scale of randomly selected hundred year segments. Thus, our simple model run with a single heat capacity, and with parameters yielding real decorrelation time scales ranging from 5 yr up to 25 yr, produces 100 yr segments within a standard deviation of the mean that have decorrelation time scales of 5 yr or less. In particular, for a 25 yr decorrelation time scale, the expected mean decorrelation time scale of a randomly selected 100 yr segment is 15 yr, with a standard deviation of 10 yr. Thus, the fact that the observed temperature time series of the last 50 yr of global temperature exhibits a decorrelation time scale of 5 yr (Schwartz, 2007), means only that the true value could be anywhere from 3 yr to 25 yr, and have the observed value within a single standard deviation of the expected value.

Second, when the model has more than a single heat reservoir, autocorrelations based on a hundred year sample can substantially underestimate both the true decorrelation time scale and the adjustment timescale. This is clear from panel Fig. 7b where the lag autocorrelation curve based on 10 000 yr of data exceeds 95% of the curves based on 100 yr segments out to 30 yr lag.

Finally we demonstrate how our simple model with a fast surface heat reservoir coupled to a large deep heat reservoir can fool the method of Schwartz (2007) into falsely ranking the climate sensitivities of the model run for various parameter choices. In Fig. 8, results in black are for parameter choices that give high climate sensitivity ($f_\alpha = f_e = 0.002$, Sensitivity: $0.4\,\mathrm{K\,W^{-1}\,m^2}$) and relatively weak coupling between the two mixed

layers $(C_s=1\times10^8\,\mathrm{J\,m^{-2}\,K^{-1}}$ (25m)$, C_{s2}=1.3\times10^9\,\mathrm{J\,m^{-2}\,K^{-1}}$ (333 m)$, \gamma=5\,\mathrm{W\,m^{-2}\,K^{-1}})$. Results in red are for parameter choices that give low climate sensitivity $(f_\alpha=f_\epsilon=-0.01$, Sensitivity: $0.1\,\mathrm{K\,W^{-1}\,m^2})$ and a single deep mixed layer $(C_s=1.3\times10^9\,\mathrm{J\,m^{-2}\,K^{-1}}$ (333 m)$, \gamma=0\,\mathrm{W\,m^{-2}\,K^{-1}})$. Panel a shows the response of each
5 model to a step change in climate forcing. The high sensitivity, weakly coupled model jumps up rapidly, but after the temperature difference between the upper and lower mixed layers increases, the flux of heat from the upper to the lower layer slows the temperature rise until equilibrium is reached. The low sensitivity, single mixed layer model approaches equilibrium at the same constant e-folding rate. Panel b shows the
10 lag autocorrelation curves for 100 100-yr segments of model output forced by noise. The lag autocorrelation curves show higher autocorrelation for the low climate sensitivity model, just the opposite of the result predicted by Schwartz (2007), even though the climate sensitivities vary by a factor of 4.

5 Discussion and conclusions

15 Some clear conclusions may be drawn from our work.

1. The FDT is poorly suited to the evaluation of model sensitivity in practice. Although it can produce precise, accurate estimates, given sufficient time, the time required for accurate evaluation of model sensitivity is in general several times longer than a model would require to come to equilibrium with a step-change in
20 forcing.

2. Estimates of climate sensitivity using real global mean temperature variations are consistent with those using output data from the 20c3m IPCC AR4 model runs. There is no inconsistency between the model climate sensitivities and the observed global mean temperature decorrelation timescales, as claimed by
25 Schwartz (2007).

3. Analysis of output from a simple climate model shows that the existence of multiple heat capacities in a climate system introduces systematic errors to the estimation of decorrelation time scale from the temperature time series. This may largely account for the systematic underestimate of IPCC model climate sensitivity by the lag-correlation method.

4. The large variability of the estimated climate sensitivity derived from these runs, even for multiple runs of the same model, confirms our prediction that estimation of climate sensitivity from a time series of a single variable requires much longer climate records than exist for the real world.

References

Bell, T. L.: Climate sensitivity from fluctuation dissipation: some simple model tests, J. Atmos. Sci., 37, 1700–1707, 1980. 12411

Callen, H. B. and Greene, R. F.: On a theorem of irreversible thermodynamics, Phys. Rev., 86, 702–710, 1952. 12411

Cionni, I., Visconti, G., and Sassi, F.: Fluctuation dissipation theorem in a general circulation model, Geophys. Res. Lett., 31, L09206, doi:10.1029/2004GL019739, 2004. 12411, 12414, 12415

Foster, G., Annan, J. D., Schmidt, G. A., and Mann, M. E.: Comment on Heat Capacity, Time Constant, and Sensitivity of Earths Climate System by S. Schwartz, in press, J. Geophys. Res., 2008 12412

Diagnosing climate sensitivity from fluctuations

D. Kirk-Davidoff

Printer-friendly Version

Interactive Discussion

Goody, R. M., Anderson, J. G., and North, G.R.: Testing climate models: an approach, Bull. Am. Met. Soc., 79, 2541–2549, 1998. 12411

Hansen, J., Ruedy, R., Sato, M., and Reynolds, R.: Global surface air temperature in 1995: Return to pre-Pinatubo level, Geophys. Res. Lett., 23, 1665–1668, 1996. Updated at http://data.giss.nasa.gov/gistemp/ 12416

Knutti, R., Krähenmann, S., Frame, D. J., and Allen, M. R.: Comment on "Heat capacity, time constant and sensitivity of Earths climate system" by S. E. Schwartz, in press, J. Geophys. Res., 2008. 12412

Langen, P. L. and Alexeev, V. A.: Estimating $2 \times CO_2$ warming in an aquaplanet GCM using the fluctuation-dissipation theorem, Geophys. Res. Lett., 32, L23708, doi:10.1029/2005GL024136, 2005. 12411

Leith, C. E.: Climate response and fluctuation dissipation, J. Atmos. Sci., 32, 2022–2026, 1975. 12411

Levitus, S., Antonov J., and Boyer T.: Warming of the world ocean, 1955–2003, Geophys. Res. Lett., 32, L02604, doi:02610.01029/02004GL021592, 2005. 12416, 12428

North, G. R., Bell, R. E., and Hardin, J. W.: Fluctuation dissipation in a general circulation model, Clim. Dynam., 8, 259–264, 1993. 12411

Penland, C. and Sardeshmukh, P. D.: The optimal growth of tropical sea surface temperature anomalies, J. Climate, 8, 1999–2024, 1995. 12413

Scafetta, N.: Comment on Heat capacity, time constant, and sensitivity of Earths climate system by Schwartz, in press, J. Geophys. Res., 2008. 12412

Schwartz, S. E.: Response to Comments on "Heat capacity, time constant, and sensitivity of Earth's climate system", in press, J. Geophys. Res., 2008. 12412

Schwartz, S. E.: Heat capacity, time constant, and sensitivity of Earth's climate system, J. Geophys. Res., 112, D24S05, doi:10.1029/2007JD008746, 2007. 12410, 12411, 12412, 12414, 12415, 12416, 12417, 12418, 12422, 12423, 12424, 12428

von Storch, J. S.: On statistical dissipation in GCM-climate, Clim, Dynam,, 23, 1–15, 2004. 12411

Title Page

Abstract | Introduction

Conclusions | References

Tables | Figures

◄◄ | ►►

◄ | ►

Back | Close

Full Screen / Esc

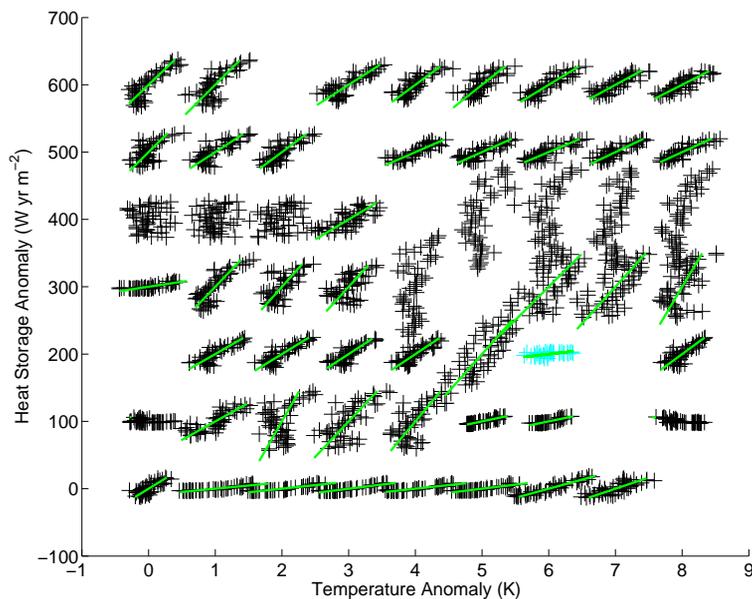Printer-friendly Version

Interactive Discussion
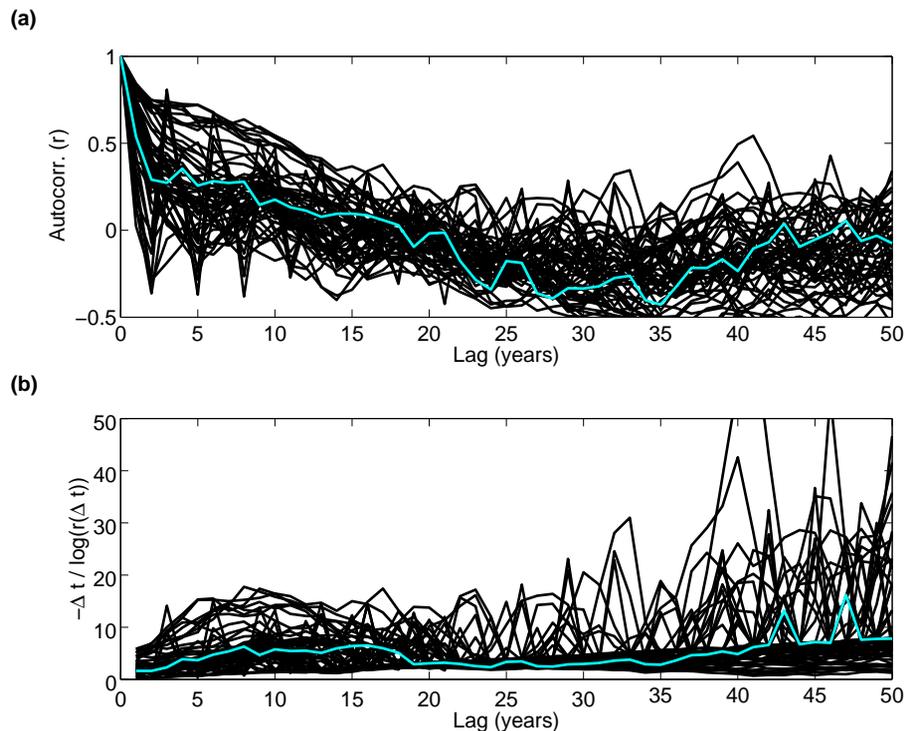
Fig. 1. (a) Lag autocorrelation of global mean temperatures from the GISS surface air temperature record (light blue), and from the IPCC AR4 20th Century runs (black). **(b)** De-correlation timescale $\tau/log(r\tau)$) for the time global mean time series, and the same color-coding.

Fig. 2. Integrated net downward surface Heat Flux (in units of W yr m^{-2}) plotted versus Global mean surface air temperature anomaly. IPCC Models output data are shown in black as in Fig. 1, with the GISS temperature and Levitus et al. (2005) heat storage figures taken by digitizing Fig. 4 of Schwartz (2007), shown in light blue. The green lines show linear regression fits of the heat storage to the temperature.
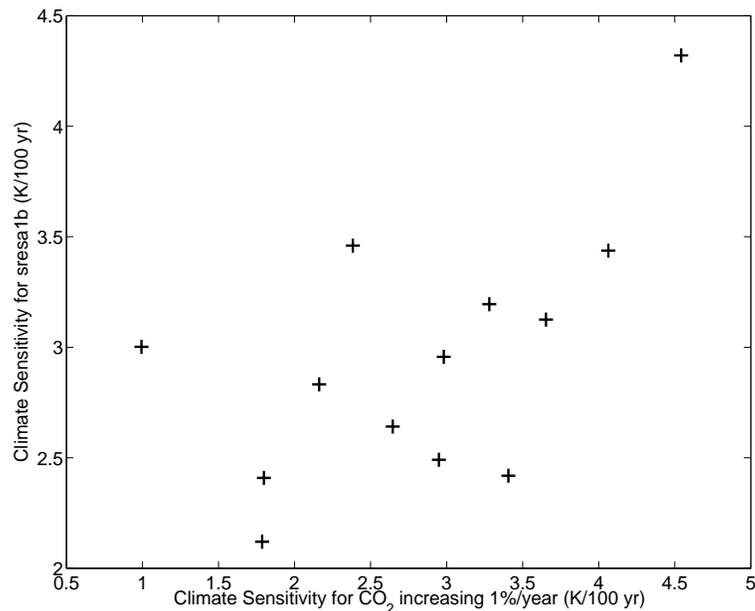
Fig. 3. Climate sensitivity from a linear fit to the first 50 yr of the IPCC AR4 runs with 1% per year increasing CO_2 versus climate sensitivity derived from the temperature difference between the years 2100 and 2100 in the SRESa1b runs.

Diagnosing climate sensitivity from fluctuations

D. Kirk-Davidoff
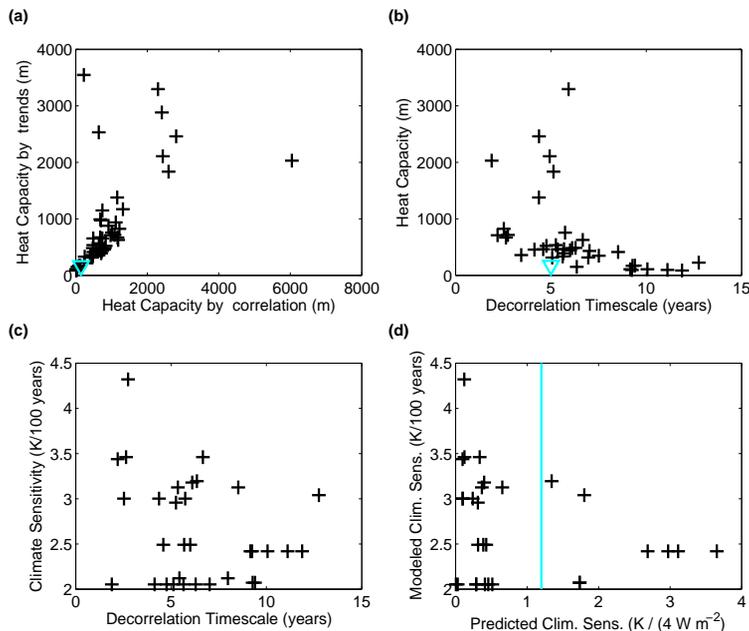
Fig. 4. (a) Scatter plot of heat capacity (in units of meters of sea water) calculated for the IPCC AR4 twentieth century (20c3m) model runs by direct correlation of heat storage and temperature versus heat capacity calculated by the ratio of the trends of heat storage and temperature over the 20th century. Colors are the same as those used in Fig. 1. **(b)** Heat capacity from the mean of the two methods used in (a) versus decorrelation time scale. **(c)** Climate sensitivity derived from the trend of the first 50 yr of the runs forced with a 1 percent per year increase in carbon dioxide versus decorrelation time scale. **(d)** Climate sensitivity predicted by the method of Schwartz (2007) from the IPCC AR4 20th century runs, versus actual climate sensitivity derived from the SRESa1b scenario temperature difference between the years 2100 and 2000. Schwartzs (2007) estimate of climate sensitivity is indicated with the light blue line.
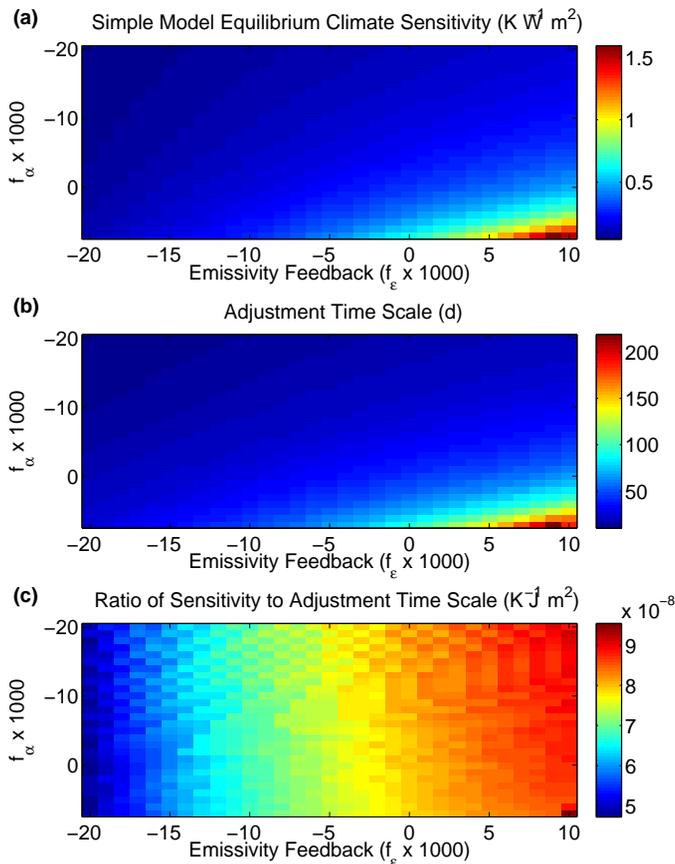
Fig. 5. (a) Equilibrium climate sensitivity of the simple climate model for a range of values of the feedback parameters f_e and f_α. **(b)** Adjustment timescale (time to 90% of response) for the same feedbacks **(c)** and for forcing by changes in the solar constant (a and c) and and in the emissivity (b and d).
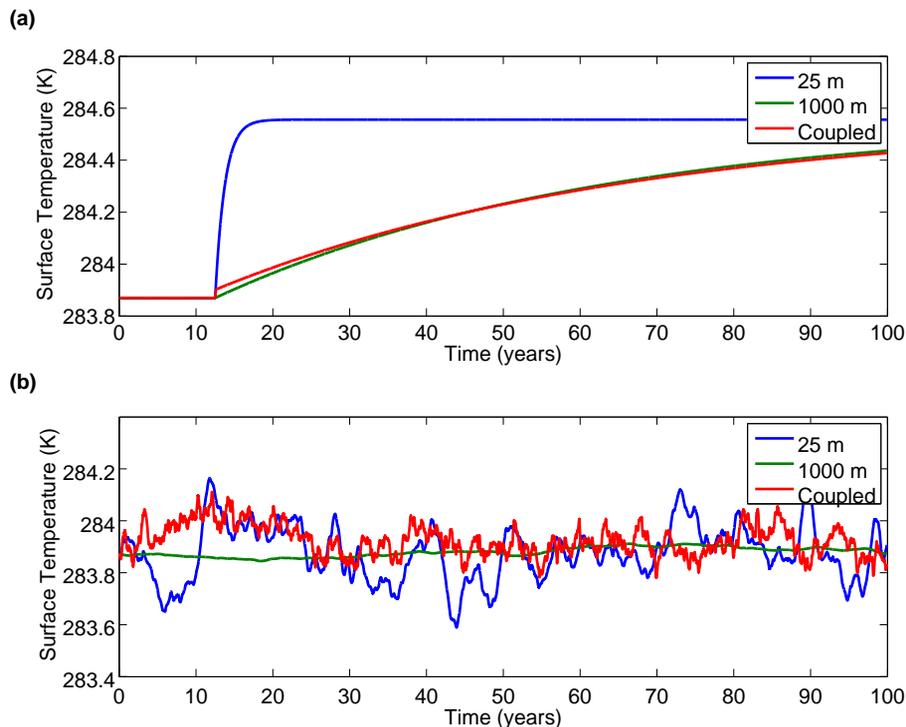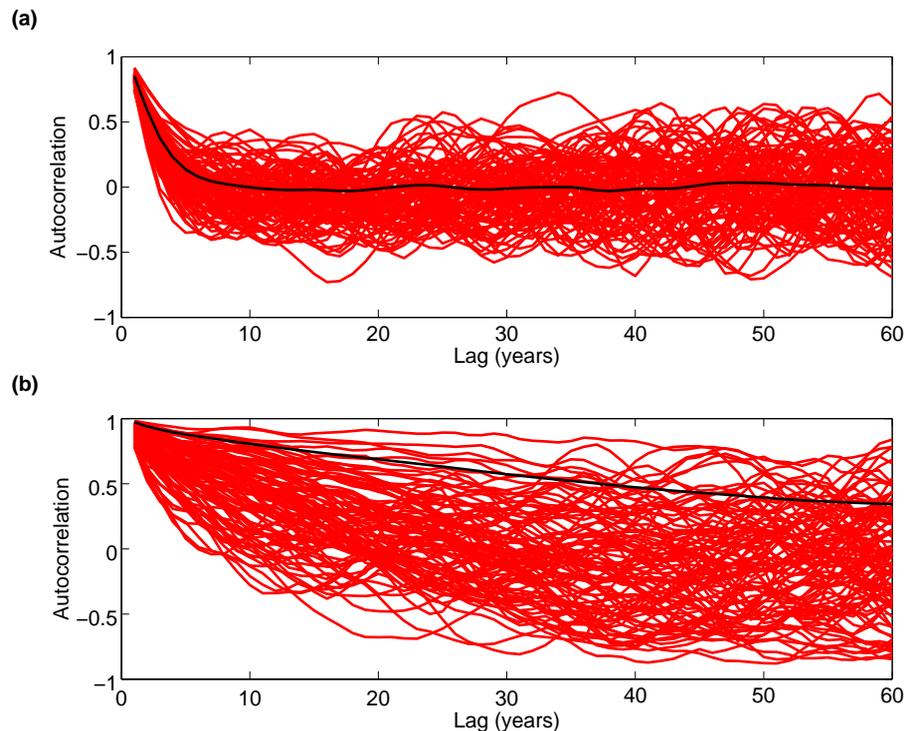
Fig. 6. (a) Response of the simple climate model to an instantaneous increase in the model solar constant for three different cases: a single 25 m ocean mixed layer (blue), a single 1000 m ocean mixed layer (green) and a 25 m ocean mixed layer coupled to 1000 m deeper mixed layer (red). **(b)** Response of the same model, with the same color-coded configurations, to random fluctuations in the solar forcing.

Fig. 7. **(a)** Lag autocorrelation for a ten thousand-year run of the simple model with a 25 m ocean mixed layer (black) and for a hundred hundred-year subsamples of the same run (red). **(b)** As for (a), for run with a 25 m ocean mixed layer coupled with a 1000 m lower mixed layer.

(a)

(b)
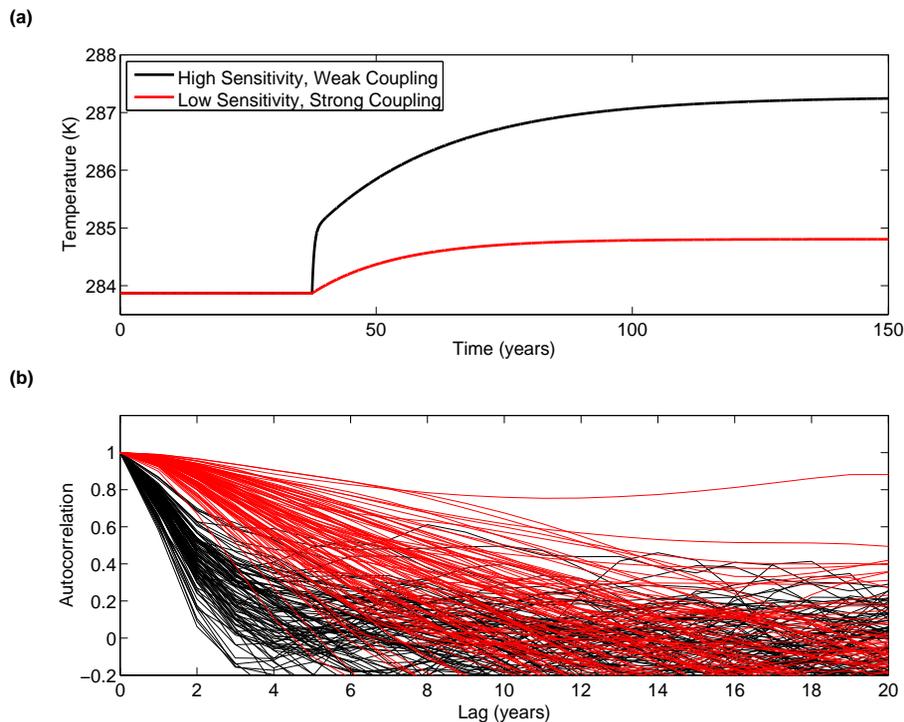
Fig. 8. (a) Response of the simple climate model to an instantaneous increase in the model solar constant for two different cases, one with low climate sensitivity and a single 1000 m ocean mixed layer, and one with high climate sensitivity and a 25 m mixed layer coupled to a 333 m deep mixed layer. **(b)** Lag autocorrelations of the surface temperature of the same two models, for 100 100- yr runs each.